

Development of Low Hysteresis, Linear Weft-Knitted Strain Sensors for Smart Textile Applications

Bozali, Beyza; Ghodrat, Sepideh; Plaude, Linda; van Dam, Joris J.F.; Jansen, Kaspar M.B.

DOI

[10.3390/s22197688](https://doi.org/10.3390/s22197688)

Publication date

2022

Document Version

Final published version

Published in

Sensors

Citation (APA)

Bozali, B., Ghodrat, S., Plaude, L., van Dam, J. J. F., & Jansen, K. M. B. (2022). Development of Low Hysteresis, Linear Weft-Knitted Strain Sensors for Smart Textile Applications. *Sensors*, 22(19), Article 7688. <https://doi.org/10.3390/s22197688>

Important note

To cite this publication, please use the final published version (if applicable). Please check the document version above.

Copyright




Other than for strictly personal use, it is not permitted to download, forward or distribute the text or part of it, without the consent of the author(s) and/or copyright holder(s), unless the work is under an open content license such as Creative Commons.

Takedown policy

Please contact us and provide details if you believe this document breaches copyrights. We will remove access to the work immediately and investigate your claim.

Article

Development of Low Hysteresis, Linear Weft-Knitted Strain Sensors for Smart Textile Applications

Beyza Bozali , Sepideh Ghodrat , Linda Plaude, Joris J. F. van Dam and Kaspar M. B. Jansen 

Faculty of Industrial Design Engineering, Delft University of Technology, Landbergstraat 15, 2628 CE Delft, The Netherlands

* Correspondence: B.Bozali@tudelft.nl; Tel.: +31-6-34362395

Abstract: In recent years, knitted strain sensors have been developed that aim to achieve reliable sensing and high wearability, but they are associated with difficulties due to high hysteresis and low gauge factor (*GF*) values. This study investigated the electromechanical performance of the weft-knitted strain sensors with a systematic approach to achieve reliable knitted sensors. For two elastic yarn types, six conductive yarns with different resistivities, the knitting density as well as the number of conductive courses were considered as variables in the study. We focused on the 1×1 rib structure and in the sensing areas co-knit the conductive and elastic yarns and observed that positioning the conductive yarns at the inside was crucial for obtaining sensors with low hysteresis values. We show that using this technique and varying the knitting density, linear sensors with a working range up to 40% with low hysteresis can be obtained. In addition, using this technique and varying the knitting density, linear sensors with a working range up to 40% strain, hysteresis values as low as 0.03, and *GFs* varying between 0 and 1.19 can be achieved.

Keywords: smart textiles; knitted strain sensors; hysteresis-free sensors; conductive yarns



Citation: Bozali, B.; Ghodrat, S.; Plaude, L.; van Dam, J.J.F.; Jansen, K.M.B. Development of Low Hysteresis, Linear Weft-Knitted Strain Sensors for Smart Textile Applications. *Sensors* **2022**, *22*, 7688. <https://doi.org/10.3390/s22197688>

Academic Editor: Sri Krishnan

Received: 22 August 2022

Accepted: 5 October 2022

Published: 10 October 2022

Publisher's Note: MDPI stays neutral with regard to jurisdictional claims in published maps and institutional affiliations.



Copyright: © 2022 by the authors. Licensee MDPI, Basel, Switzerland. This article is an open access article distributed under the terms and conditions of the Creative Commons Attribution (CC BY) license (<https://creativecommons.org/licenses/by/4.0/>).

1. Introduction

With the recent interest in wearable technology, it has become increasingly important to have textile-based sensors that can be a potential platform for future applications and products. Textile-based sensors are essential components of wearable technology due to their flexibility, breathability and ease of application, and therefore can be used in many different applications, such as monitoring heart rate, pulse and other health signals [1], generating human-machine interface systems [2] and producing textile-based systems for electromagnetic interference shielding (EMI) purposes [3]. Textiles with embedded strain sensors can measure local movements of body parts and can be used to monitor posture and limb locomotion but also e.g., respiration. Related applications include sensor gloves and VR suits as well as elbow and knee revalidation aids and sensory compression garments.

A strain sensor is an electronic device that produces an electrical signal in response to mechanical deformation [4]. Typical strain sensors used for engineering purposes consist of thin metal layers on a polyimide substrate and have a working range which is limited to about 1%. Those types of sensors are therefore inadequate to detect movements of the skin or the clothing layer attached to it which may range up to 40% [5]. Textile-based strain sensors offer a new generation of devices that combine strain sensing functionality with wearability, lightness and high stretchability. They can be comfortably worn and sense a wide range of body strains for a vast number of applications.

Textile-based strain sensors can be produced with standard textile manufacturing methods such as knitting [6], embroidering [7], or stitching [8]. For stitched and embroidered sensors, the response of sensors is determined by the stitch structure and as well as the base fabric characteristics, and therefore the elastic response of the substrate is critical to achieving reliable sensors. Knitted structures are good candidates for designing flexible strain sensors thanks to their high stretch recovery and good stretchability

characteristics [9]. The main advantage of knitted sensors is that they can be manufactured at low costs in mass production with existing textile equipment and readily available yarns. In addition, the sensors will be washable, breathable, and stretchable while having a fully textile appearance.

The basic working principle of knitted strain sensors can be explained by loops of conductive yarn embedded in overlapping and adjacent rows. During stretching, the points of contact alter, causing the overall resistance to change. This resistance change is reproducible, and if large enough, it can be used as a sensor signal [10]. The human skin typically deforms up to 40% [11] which thus defines the desired upper limit of body strain sensors [12]. For breathing rate measurements, the strains are in the order of 5%. A useful knitted sensor should thus ideally have a working range up to 40% and a resolution of about 1%. In addition, strain sensors for on-body monitoring should be linear and have negligible hysteresis.

The performance of knitted strain sensors is affected by two parameters, one is the material type and the other is the knitting structure. Considering the material type, the effect of elastic or conductive yarns on sensor performance comes to the fore. The embedded structure in a knitted sensor must be highly elastic as it determines the effects of time lag and hysteresis and this elasticity is provided by elastic yarns containing lycra or elastane [13,14]. A study by Atalay pointed out that the properties of elastomeric yarn had a significant impact on the performance of the sensor [10]. In addition, the use of covered elastic yarn instead of bare elastic yarns has resulted in higher sensitivity [15]. Conductive materials are another important determinant of sensor performance. Metallic yarns such as stainless steel-based conductive yarns showed an unstable performance in many studies which was attributed to shortcuts caused by loose yarn filaments. On the other hand, yarns consisting of stainless steel fibers blended with cotton appeared to show improved performance with better sensitivity than sensors knitted with commercial metalized polyamide multifilament yarn due to more stable contact resistance [16]. In contrast to metallic yarns, silver-based nylon yarns show stable electromechanical performance. Although silver-based nylon yarns are capable of producing high sensitivity sensors, the hysteresis values of the sensors can vary from structure to structure and remains a challenge to optimize for reliable sensors. Liang et al. also remark that a promising way to reduce hysteresis is to use Eeontex in the sensor base structure [14]. The resistivities of the currently available conductive yarns vary widely, and the study of Raji et al. [17] seems to suggest that sensors with conductive yarn with a resistance of 77 ohm/cm have an optimum GF in the resistance range of 40 to 120 ohms, but the effect was not studied in detail [18]. The type of knit design is another essential parameter that affects the sensor performance, and many different studies to investigate the effect on sensor performance were reported. One is a single jersey knit strain sensor, developed by adding float and crimp stitches to a structure knit that appears to be suffering from relatively large hysteresis effects [19]. Interlock structures knitted with conductive yarns show a good sensor performance having a gauge factor (GF) value of 3.5 at between a 10–40% working range. In the case of 1×1 rib knitted samples, the effect of the aspect ratio and shape of the sensing region was evaluated by Raji et al. and they concluded that plain rectangular sensors showed higher repeatability and lower noise levels compared to non-rectangular shaped sensors [15]. A 1×1 rib knit design was found to be promising as a strain sensor and presented a sensor with a GF of 1.36 and a working range of 0–21% by Chia et al. [20].

Various materials and methods in the design of knitted strain sensors have been reported so far but until now are not reliable, and linear and low-hysteresis sensors were reported. In our quest to develop such sensors we take the findings of previous studies, summarized below as a starting point:

- Steel-based conductive yarns are less suitable for strain sensors because of the relatively high noise levels associated with knitted sensors and silver coated nylon yarns should be preferred accordingly [16,21].

- Next, the base fabric in which the sensor yarns are embedded needs to be fully elastic. If not, the sensor will not respond elastically and will be prone to show time lag and hysteresis effects [14].
- Rib structures as knit design allow for stretching abilities up to 100% and are therefore potential strong candidates for knitted strain sensors [17].
- Sensors should preferably be rectangular with aspect ratios between 24:1 to 77:1 [17].

In the current paper, we take these conclusions as a starting point and report a systematic study on the performance of knitted strain sensors to develop reliable strain sensors with high sensitivity, wide working range and low hysteresis. We do this by manufacturing a series of sensors with the elastic and conductive yarn types as variables, the number of conductive courses, the knit density, and the conductive yarn position in a co-knitted configuration. The electromechanical performance is evaluated by determining the initial resistance, sensitivity, working range and hysteresis for all knitted sensors. Based on these sensor constructions, knitted sensors with minimum hysteresis, maximum sensitivity and working range are selected and evaluated.

2. Materials and Methods

Based on the above-mentioned observations from the literature, the following initial choices are made: (i) A rectangular sensor area consisting of a number of parallel conductive courses, (ii) A 1×1 rib knit design, (iii) Silver-coated or plated nylon as the conductive yarn, and (iv) Elastic yarn with as high elastic recovery as possible. As elastic yarns, we used the ones provided by Yeoman (Nm 13, 81% Nylon and 19% Lycra) and Uppingham (Nm 11, 16.74% Lycra and 83.26% Nylon). As conductive yarns, six different silver-coated nylon yarns with various resistivities from Amann Threads UK Ltd. (Ashton-under-Lyne, UK) and Shieldex, Statex Productions- and Sales GmbH (Bremen, Germany) were selected (See the optical images of the conductive yarns in Figure S1). The property details and related coding of these yarns are listed in Table 1.

Table 1. Conductive yarn details and related properties.

Composition	Coding	Linear Density (Dtex *)	Resistivity (Ω/m)	Manufacturer
Silver coated polyamide/ polyester hybrid yarn	A1	960	85	Amann
	A2	620	150	
	A3	280	530	
Silver plated polyamide 6 yarn	S1	235	600	Shieldex
	S2	117	1500	
	S3	78	3500	

* The weight per 10,000 m (dtex) reflects the yarn thickness.

In weft knitted fabrics, the horizontal row of continuously connected loops is called a course, whereas the series of loops that intermeshes vertically is known as wales, as illustrated in Figure 1a. In this study, knitted strain sensors have been produced on a Stoll CMS 530 flatbed knitting machine with a gauge of E8. An 1×1 rib knit structure was chosen for all samples. The conductive yarn is co-knitted with a non-conductive elastic yarn using a yarn carrier with two eyelets as shown in Figure 1b. In that way, the position of the conductive yarn with respect to the elastic support yarn is well controlled, resulting in a rib structure in which the conductive yarn is always on the inside or always on the outside. A more detailed explanation is given in Section 3.4. In order to enhance the elasticity, the base fabric was also manufactured with two parallel elastic yarns. All sensor samples have outer dimensions of approximately 14.5×7 cm. The size of the conductive area changes according to the number of conductive courses, which varied between 1 to 5.

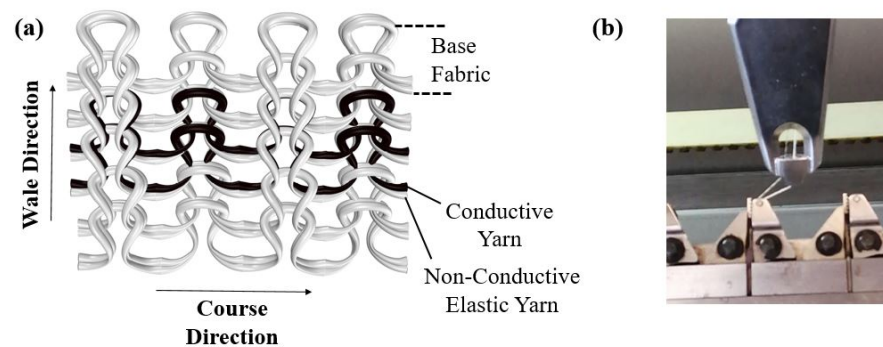


Figure 1. (a) Co-knitted 1×1 rib structure with two conductive yarn courses: (indicated in black) and non-conductive yarns (white), and (b) A yarn carrier containing two parallel yarns.

Knitted strain sensors were prepared with the parameters listed in Table 2. The conductive course number was varied between 1 to 5, and knit densities were varied by selecting NP numbers between 6 to 15. The NP value is related to the needle pitch distance. The position of the conductive yarn is referred to as conductive outside (CO) and conductive inside (CI), respectively. This will be discussed in detail later (see Figure S2).

Table 2. Parameters of knitted strain sensors tested in the study and the section in which they are discussed.

Parameters	Variations	Section
NP number	6, 7, 8, 9, 10, 12 and 15	Section 3.2
Conductive yarn type	Shieldex (S_1, S_2, S_3) and Amann (A_1, A_2, A_3)	Section 3.5
Conductive course number	1, 2, 3, 4 and 5	Section 3.5
Elastic yarn type	Yeoman (E_1) and Uppingham (E_2)	Section 3.3
Configuration of the c. yarn	Inside (CI) and Outside (CO)	Section 3.4

In this paper, knitted samples will be coded as $NP_x Y_x C_x E_x$ following all the parameters listed in the Tables 1 and 2. As an example, $NP_{10} Y_{S1} C_2 E_1$ can be interpreted as the sample knitted with a NP setting of 10 and with two conductive courses using S_1 conductive and E_1 elastic yarns, respectively.

2.1. Resistance-Strain Testing Procedure

The electromechanical properties of the knitted strain sensors were investigated by measuring the changes in resistance during cyclic tensile tests in which the sample was subsequently loaded and unloaded. A custom-made tensile tester with a 1000 N load cell was used to generate a cyclic stretching between 0–40% at a constant speed of 30 mm/min as depicted in Figure 2. The samples were stretched in the course direction. Preliminary testing showed that test speed did not have a large effect on the performance in terms of sensitivity and working range in Table S1. The initial length of the samples known as the gauge length was set at 50 mm. All tests were conducted in standard atmospheric conditions. The resistances were measured using a 4-point probe method in which a constant current value of 0.3 mA was applied to the outer red clamps in Figure 2. The resulting voltage drop was read from the inner dark green electrodes and stored in a data acquisition system. The resistance values were calculated as the ratio between measured voltage and current values. Mechanical clamps with conductive Velcro tape were used to clamp the samples and provide the electrical connection.

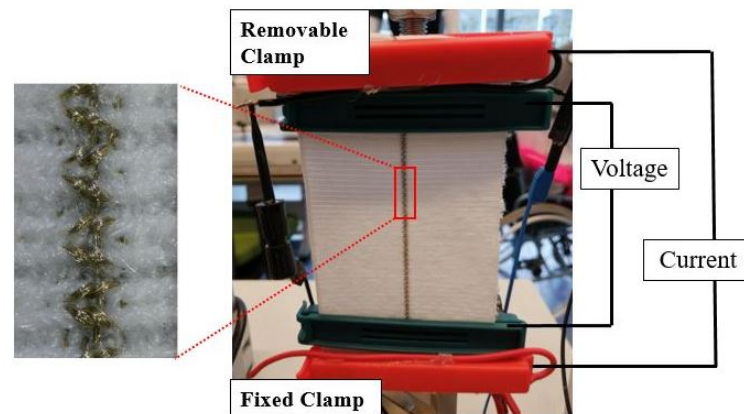


Figure 2. Test setup with an attached knitted strain sensor and four-point probe connections.

2.2. Electromechanical Properties

The electromechanical properties such as gauge factor GF , working range WR and hysteresis were investigated to analyze the performance of the knitted sensors. During the stretching of sensors, the resistance does not always change monotonically. Thus not all parts of the recorded resistance changes are suitable to indicate the sensor performance. We define the working range as the region in which the resistance changes monotonically. The onset and end of the working range are referred to ϵ_{max} and ϵ_{min} , respectively (see Figure 3a). The working range (WR) is then defined as (Equation (1));

$$Working\ Range(WR) = \epsilon_{max} - \epsilon_{min}, \quad (1)$$

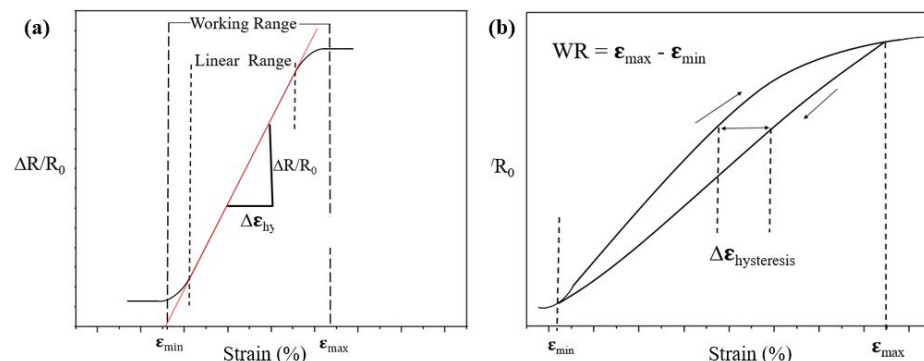


Figure 3. (a) A graph showing how to calculate the gauge factor and working range, and (b) A graph showing how to calculate the resistance hysteresis (Black arrows represent the loading and unloading during a cycle).

The GF or sensitivity is defined as the slope of the linear range of the relative resistance change versus the applied strain graph as can be seen in Figure 3a. Equation (2) shows the formula for the gauge factor in which $\Delta R = R_{Stretched} - R_0$, R_0 is the initial resistance, and $\Delta \epsilon$ is the strain change within the linear region of the curve.

$$Gauge\ Factor(GF) = \frac{(\Delta R/R_0)}{\Delta \epsilon}, \quad (2)$$

Hysteresis values can be calculated along the resistance axis (vertical) or along the strain axis (horizontal), and these values will be referred to as *resistance hysteresis* and *strain hysteresis*, respectively [18]. For a strain gauge in an application, the expected errors in the measured strain are of primary concern; thus, as a performance indicator, we prefer to use the strain hysteresis values and not the more commonly reported resistance hysteresis [22,23]. When the maximum strain in a loading cycle increases, it is evident that

the hysteresis also increases. Since we prefer the hysteresis values not to depend too much on the loading conditions, we choose to scale the hysteresis with the working range as shown in Equation (3) and Figure 3b. The hysteresis strain, $\Delta\varepsilon_{\text{hysteresis}}$, can be defined as the maximum difference between loading and unloading strain as shown in Figure 3b.

$$H_\varepsilon = \frac{\Delta\varepsilon_{\text{hysteresis}}}{WR}. \quad (3)$$

3. Results

3.1. Electromechanical Performance Analysis of a Knitted Strain Sensor

As a first example, we discuss the NP₁₀ knitted sample test as shown in Figure 4.

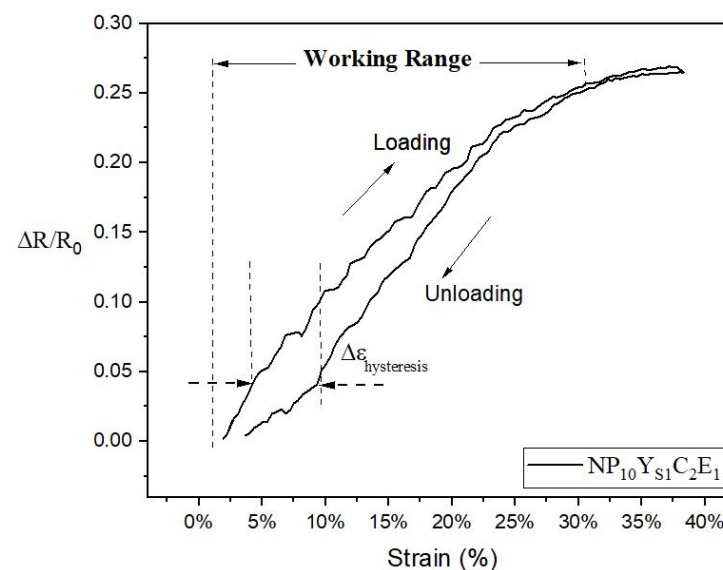


Figure 4. Relative resistance change versus strain plot of knitted strain sensor type NP₁₀Y_{s1}C₂E₁.

During stretching up to 40%, the relative resistance of the sample changes from 0 to a value of 26%. The last part of the stretching curve shows that the amount of increase in the resistance gradually decreases. During the first part of the unloading curve, the resistance roughly follows the curve of the loading cycle, but deviations start below about a 20% strain, leading to hysteresis. At the end of the unloading cycle, the resistance change approaches nearly its starting value. For this experiment, the working range, gauge factor and hysteresis are determined as $WR = 0\text{--}27\%$, $GF = 0.89 \pm 0.06$, and $H = 0.07$, respectively.

As previously explained in Section 2, knitted sensors were fabricated by making conductive/elastic yarn combination. Knitted sensors without elastic support yarn were also investigated to better understand the effect of using elastic yarn as a co-knit yarn in the sensing region. The results showed that the sample without the co-knitted elastic yarn had a nearly strain-independent resistance where GF was close to -0.1 , which can be seen in Figure S3. A gauge factor below zero means that the resistance drops when the sample is stretched. Configurations with gauge factors close to zero may prove useful as stretchable interconnects in knitted textile circuits.

3.2. The Effect of Knit Density (NP Number) on the Sensor Performance

Knitted densities are determined by the NP numbers. A higher NP number results in less dense fabric structures, while lower NPs result in denser fabrics. Optical images of the NP_xY_{s1}C₂E₁ series are shown in Figure 5. Areal densities (g/m^2) of the knitted fabrics are calculated using Equation (4) in which YL is the yarn length in a knit design (mm), LD denotes the linear density in Tex, WS is the wale spacing in mm, CS the course spacing in mm, S_h : horizontal size, and S_v : vertical size [24]. The yarn length was determined by unraveling the course of the fabric and measuring the distance when stretched.

$$\text{Areal Density} = \frac{YL \times LD}{WS \times S \times S_h \times S_v} \quad (4)$$

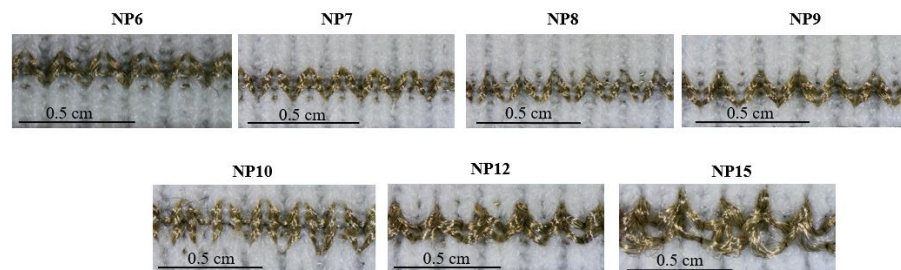


Figure 5. The optical images of knitted strain sensors of the series of $NP_x Y_{S1} C_2 E_1$.

The optical images show that, when the NP number increases, the samples become looser and less dense, an observation which is conformed by the decrease in areal density in relation to the NP numbers as can be seen in Table 3. Accordingly, the conductive yarns in the sensing area do not fully integrate into the structure when the NP numbers increase from NP₁₀ to NP₁₅, which could play an active role in the sensor performance in terms of the elastic recovery.

Table 3. The areal density and elastic modulus of the knitted sample series of $NP_x Y_{S1} C_2 E_1$.

NPs	Areal Density (g/m ²)	Nominal Thickness (mm)	Elastic Modulus (MPa)
6	796	1.57 ± 0.02	0.26 ± 0.01
7	614	1.57 ± 0.03	0.24 ± 0.02
8	551	1.76 ± 0.01	0.21 ± 0.005
9	402	1.74 ± 0.01	0.15 ± 0.01
10	331	1.84 ± 0.01	0.12 ± 0.01
12	216	2.27 ± 0.005	0.06 ± 0.005
15	148	2.53 ± 0.005	0.03 ± 0.002

The electromechanical performance of the strain sensors knitted with different NPs changing from NP₆–NP₁₅ is shown in Figure 6 along with *GFs* and working ranges. Tighter structures knitted with the NP numbers 6, 7, and 8 have a working range between 0–10%; above that strain value, the performance of sensors becomes unstable and nonlinear (see Figures S4 and S5). The response curve for the NP₉ sensor showed an initial minimum resistance of 15.5 ohms, hence the effective working range did not start at 0 but at a 6% strain. Similar to the working range, the gauge factor values are relatively low and range between 0.20 and 0.33. However, for less dense sensors, the gauge factors improve significantly and range from 0.70 to 1.91 as the NP number changes from 9 to 15. When the NP numbers increased from NP₉ to NP₁₅, the working range became broader.

Table 3 shows the areal density and measured elastic modulus (*E*) of the knitted samples with several NP numbers. Nominal thickness values were calculated by following the standard of BS 2544:1954—determination of thickness of the textile fabric. By using the Heidenhain length gauge, fabric samples were placed between two glass plates and fabric thicknesses were calculated by subtracting the total thickness from the previously measured glass plate thickness. The elastic modulus values were calculated by averaging over three tests. The results show that the areal density values decrease with the increase in the NP number. With an increase in NP number from 6 to 15, the areal density decrease with a factor 5.4, the fabric thickness increases 1.6 times and the modulus decreased with a factor 8.7. It demonstrates that, with higher NP numbers, we obtain more open structures

with a lower areal density and a lower elastic modulus and, as seen in Figure 6, an increased working range and gauge factor.

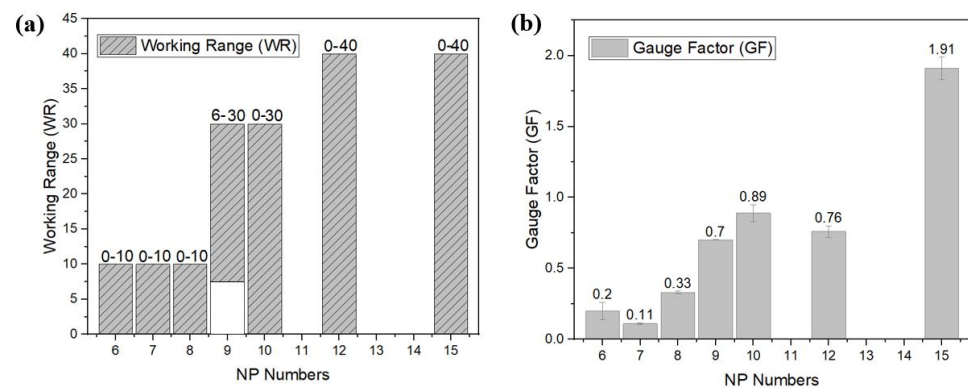


Figure 6. The effect of NP values on the sensor performance for the series of $NP_x Y_{S1} C_2 E_1$ (a) working range, and (b) gauge factor.

3.3. The Effect of an Elastic Yarn Type on Sensor Performance

The hysteresis of knitted strain sensors is known to be directly related to the ability of mechanical recovery of the sample. Therefore, in this section, we investigate the effect of elastic yarn type on sensor performance by separately comparing the performance of sensors with elastic yarns of type E_1 and E_2 . The test results are summarized in Figure 7. Although both yarns still have hysteresis, the samples knitted with E_1 yarn appear to be more promising for each NP numbers except NP_8 . Due to their higher elastic recovery performance and relatively lower hysteresis values in comparison with the E_2 yarn, for all next samples, the E_1 type yarn was used. In addition, we choose to select the NP_9 as the preferred density setting in all subsequent tests. Even though the sensor knitted with NP_7 and NP_{10} show the lowest hysteresis, a larger improvement in hysteresis was achieved for the NP_9 sample with the manufacturing technique we used for low-hysteresis sensors and the NP_9 sample seems to be more promising. This will be discussed at later stages in more detail.

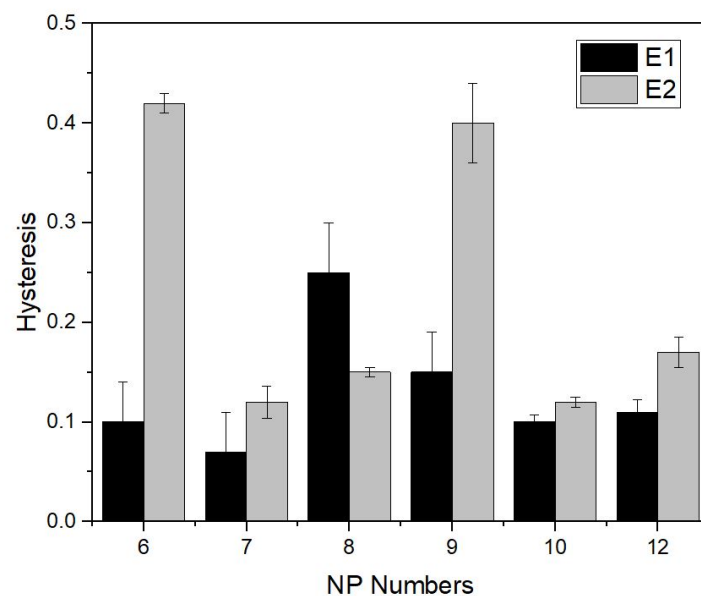


Figure 7. The effect of elastic yarn type (E_1 and E_2) on hysteresis for the series of $NP_x Y_{S1} C_2 E_1$ and $NP_x Y_{S1} C_2 E_2$. (Hysteresis is calculated according to Equation (3)).

3.4. The Effect of Conductive Yarn Configuration on the Sensor Performance

As explained in Section 2, we knitted the conductive yarns together with an elastic support yarn. By switching the position of elastic and conductive yarns in the yarn carrier, we can control whether the conductive yarn always ends up on top or below the elastic yarn (see Figure S6). For a standard jersey knit, this would result in one fabric surface with mainly conductive yarn and one with a mainly elastic yarn. The 1×1 rib structure that we use in this study, however, creates a more complex structure in which, in an unstretched state, the conductive yarns end up either at the inside or the outside of the fabric. In this section, we will investigate how that positioning affects the sensor performance. Whether the conductive yarn has been positioned inside or outside, the knit structure will be referred to as CO and CI. Examples are shown in Figure 8.

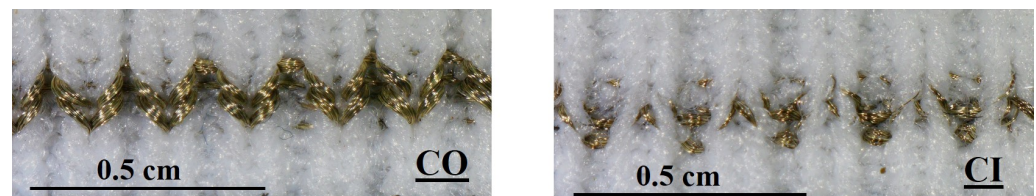


Figure 8. The yarn configuration of two samples (a) $\text{NP}_9\text{Y}_{51}\text{C}_2\text{E}_1\text{CO}$ and (b) $\text{NP}_9\text{Y}_{51}\text{C}_2\text{E}_1\text{CI}$.

The comparison of $\text{NP}_9\text{Y}_{51}\text{C}_2\text{E}_1\text{CO}$ and $\text{NP}_9\text{Y}_{51}\text{C}_2\text{E}_1\text{CI}$ samples in terms of electromechanical performance is illustrated in Figure 9. Preliminary experiments showed that, for all knitted samples, the first resistance cycle always deviated significantly which was attributed to an initial rearrangement of the knitted structure. Therefore, in all subsequent graphs, the first cycle will be omitted. In Figure 9, the resistance change graphs of both a sample with the conductive yarns outside (CO, Figure 9a) and one with the yarn inside (CI, Figure 9b) are presented. This clearly shows that the CI sample performs significantly better regarding hysteresis and linearity. The working range changes from 4–32% for the CO sample to 0–40% for the CI variant. In addition, the resistance increases almost linearly over the full working range for the CI sample, whereas the resistance change flattens out above about 28% in the case of the CO sample. Additionally, the *GF* of the CI sample, 1.19 ± 0.04 , is higher than that of the CO knitted sensor with a value of 0.70 ± 0.002 . The most significant difference was observed in the hysteresis values, which shows a sharp decline from 0.15 to 0.03 of CO and CI, respectively. The graphs show data from four subsequent cycles (cycles 2 to 5), which can be seen to be nicely overlapping indicating that at least during these initial tests the gauges showed negligible drift.

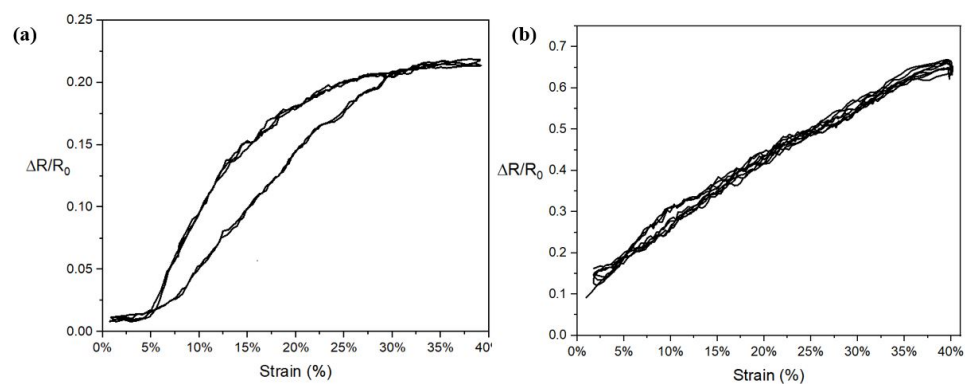


Figure 9. The two different results of samples knitted with conductive outside (a) $\text{NP}_9\text{Y}_{51}\text{C}_2\text{E}_1\text{CO}$ and conductive inside (b) $\text{NP}_9\text{Y}_{51}\text{C}_2\text{E}_1\text{CI}$.

The electromechanical performance of the $\text{NP}_9\text{Y}_{51}\text{C}_2\text{E}_1\text{CI}$ and $\text{NP}_9\text{Y}_{51}\text{C}_2\text{E}_1\text{CO}$ sensors at high strain values was also investigated and compared by testing the sample up to 70%

strain to determine the maximum of the working range. The resistance versus strain graph is depicted in Figure 10. Figure 10a shows that the resistance change levels-off between strain values 40% and 70%, indicating an overall working range of 0–40% when the conductive yarn is inserted inside. Figure 10b shows the nonlinear behaviour of the CO sample with a higher hysteresis when the deformation is applied.

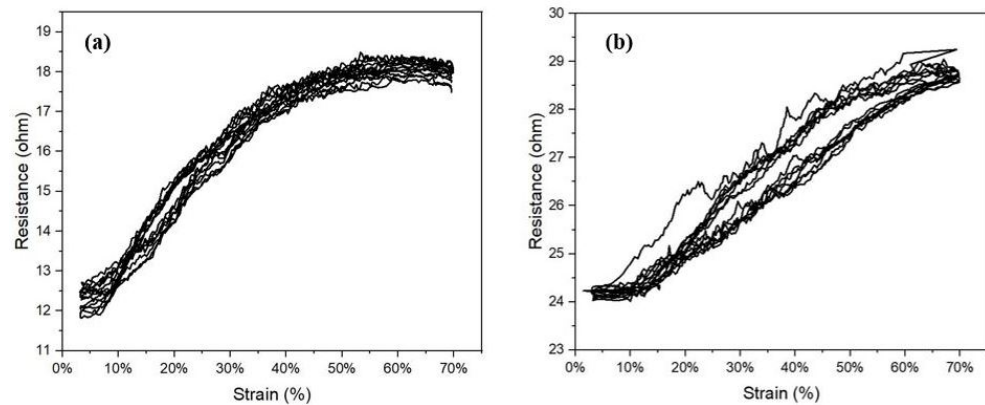


Figure 10. The electromechanical behaviour of the (a) $\text{NP}_9\text{Y}_{51}\text{C}_2\text{E}_1\text{CI}$ and (b) $\text{NP}_9\text{Y}_{51}\text{C}_2\text{E}_1\text{CO}$ sensor sample at a 70% strain value over eight applied cycles.

3.5. The Effect of Conductive Yarn Type and Conductive Course Number on Sensor Performance

Knitted strain sensors were produced using Shieldex (S) yarns with conductive course numbers ranging from 1 to 5 with a fixed NP_9 setting and both conductive inside (CI) and outside (CO) structures. The results of both S_1 and S_2 samples were illustrated in Figure 11 with gauge factor and hysteresis values. The average and corresponding error bars are presented to indicate the spread in data. For 1-course samples of S_2 , only a single measurement was available, and consequently no error value was reported. In Figure 11a,c, the gauge factor is plotted versus the number of conductive courses using conductive yarn type S_1 and S_2 , respectively. In all cases, the conductive inside (CI, grey bars) configuration resulted in the highest gauge factor values, with the effect being largest for the S_2 yarn (Figure 11c). For both yarn types, 4-course samples appear to be the optimum, resulting in GF values of 1.92 ± 0.24 and 2.10 ± 0.22 for S_1 and S_2 , respectively.

The corresponding hysteresis values are plotted in Figure 11b,d. Once again the conductive inside configuration produces the best results with lowest hysteresis values. For S_1 yarn, the change from CO to CI results in a drop in hysteresis from about 0.14 on average for the CO samples to about 0.06 for the CI samples. The lowest hysteresis values are close to $H_\varepsilon = 0.04$ and are observed for a 2-course sample (S_1 yarn, CI) and 3- or 4- course samples (S_2 yarn, CI). Note that these values are scaled to the working range, according to our definition in Equation (3). As a result, the configuration in which the conductive inside improves the performance not only for the specific knitted sample discussed in Section 3.4, but also for different conductive yarns and course numbers.

By comparing Figure 11b,d, it shows that the hysteresis value is not much affected by the number of conductive courses and always stays at a relatively high value of around 0.16 for CO samples with the S_1 yarn and around 0.20 for the S_2 yarn.

After evaluating the effect of yarn positioning on sensor performance for the S_1 and S_2 yarns of Shieldex for both CI and CO samples, the question was to explore if the conductive course numbers have an effect on CI samples knitted with Amann yarns. Samples were prepared and compared with six different conductive yarns with the yarn specifications listed in Table 1. For the comparison, only 1- and 2-conductive course numbers were prepared with CI samples and all samples, were knitted with the NP_9 setting. The gauge factor versus initial resistance plots are shown in Figure 12.

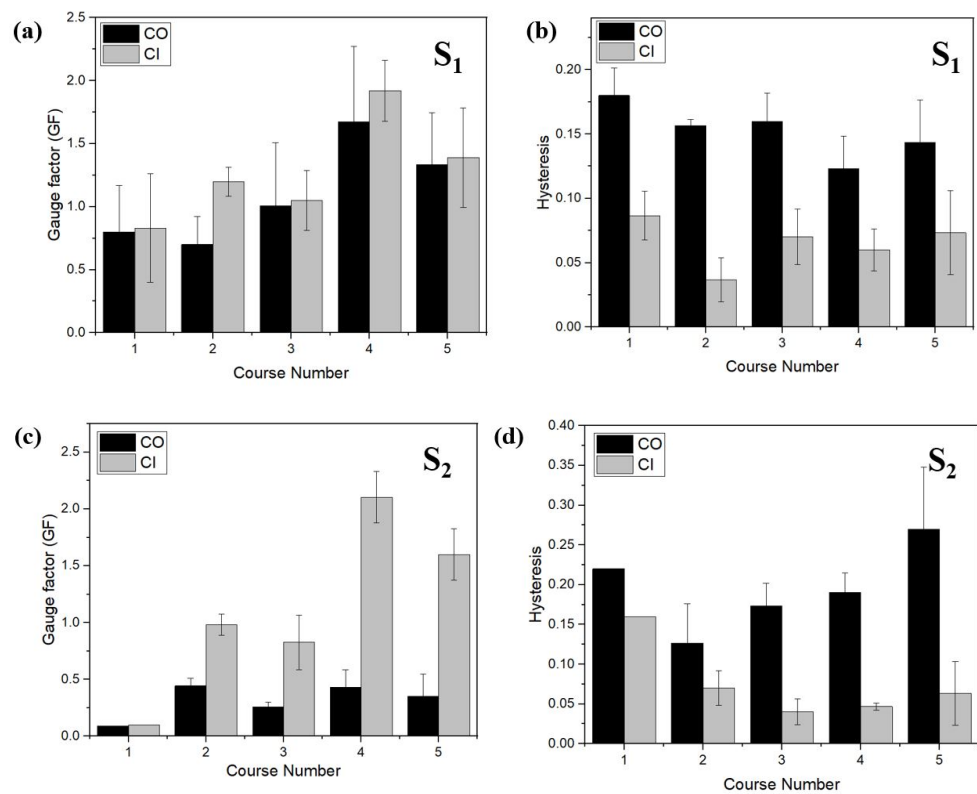


Figure 11. Effect of course number and yarn position S_1 yarn and S_2 yarn, respectively; (a) Gauge factor vs course number, (b) Hysteresis vs course number, (c) Gauge factor vs course number, and (d) Hysteresis vs course number.

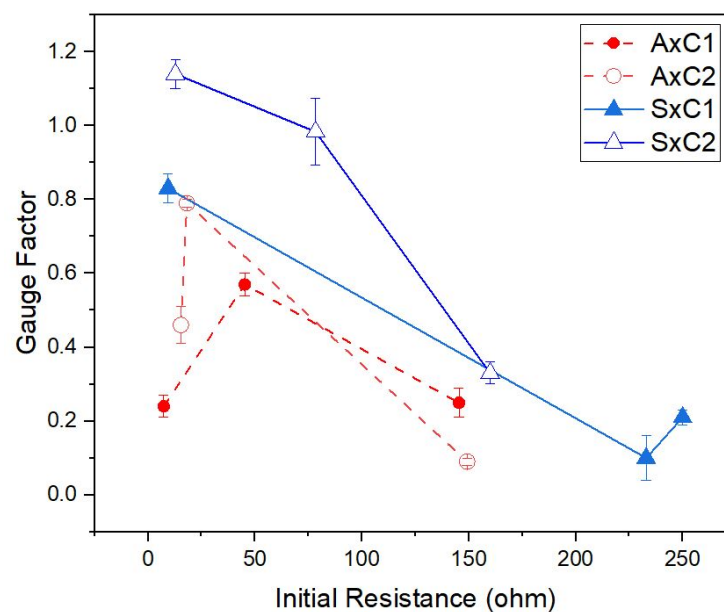


Figure 12. Gauge factor versus initial sensor resistance plots of sensors knitted with conductive yarn inside (CI) and NP₉; Sensors knitted with Shieldex yarns (S_1 , S_2 and S_3) are indicated with blue straight lines, and Amann yarns (A_1 , A_2 and A_3) with red dashed lines.

The general trend is that the gauge factor decreases with increasing the initial resistance (R_0). The major deviation from this trend is for the A_1 yarn, which shows a relatively low GF at low initial resistances for both 1- and 2- conductive course samples. It should be

noted that yarn A_1 is much thicker than the support elastic yarn E_1 , which has a thickness of 0.39 ± 0.02 mm, and this may have affected the stability of the configuration during co-knitting (see Figure S7 and Table 4).

Table 4. The yarn thicknesses and electromechanical performance of sensors knitted with NP_9 and CI/CO configurations.

Yarn Type	Yarn Thickness (mm)	Gauge Factor	
		CO	CI
A1	0.49	0.24	0.46
A2	0.33	0.57	0.79
A3	0.27	0.25	0.09
S1	0.32	0.70	1.19
S2	0.19	0.44	0.98
S3	0.16	0.21	0.33

Overall, it can be seen that 2-course samples showed better sensitivity in comparison with the 1-course samples. Thinner yarns with high resistivity such as S_2 and S_3 show a relatively poor sensing performance with GF values below 0.4. The highest GF observed is that for the 2-course configuration of the S_1 yarn around 1.19 and A_2 around 0.79. Note that low initial resistances result in higher power consumption, which can be important in practical applications for smart textiles [13].

4. Discussion

The electromechanical performance of knitted strain sensors was studied for different knitting densities, elastic/conductive yarn types, course number and elastic/conductive co-knit configurations. The sensing performance of the knitted strain sensors was evaluated with the main focus on gauge factor and hysteresis. As it can be seen from Figure 13, by varying the NP number (knitting density), we have control over the sensitivity while still being able to keep the hysteresis low.

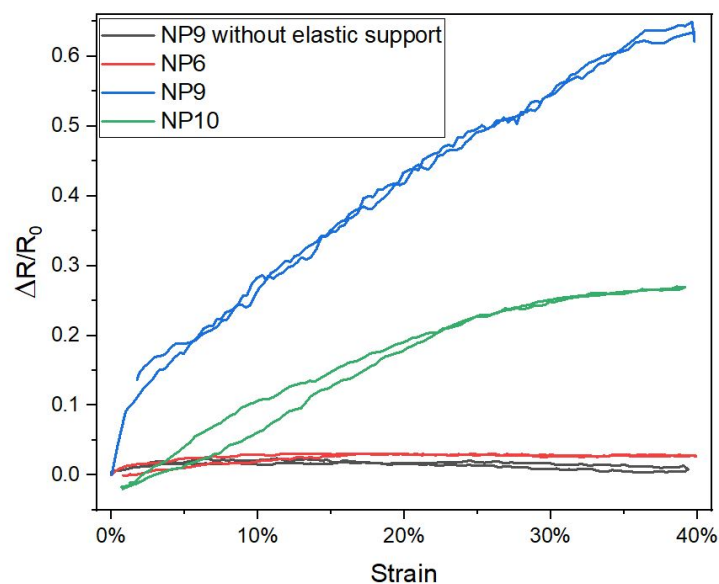


Figure 13. Different graphs showing high and low hysteresis knitted samples; $NP_9Y_{S1}C_2$ —without E_1 , with NP_6 , NP_9 and NP_{10} .

The gauge factors corresponding to the curves for NP_6 , NP_9 and NP_{10} are 0.20 ± 0.06 , 1.19 ± 0.04 and 0.89 ± 0.06 , respectively. Note that knitted conductive yarn structures with gauge factors close to zero could be of large practical importance as a basis for stretchable

interconnections between sensors and data processing units in a smart garment application. The ability to control the strain sensitivity as shown in Figure 13 thus would enable future researchers to knit a garment with a network of connected sensor elements in one go and on one machine. Note that a stretchable conducting line with zero gauge factor could also be obtained by omitting the elastic support yarn in the co-knit structure (see the black line in Figure 13).

The role of the elastic support yarn below the conductive component is therefore probably to provide enough contact pressure between overlapping loop segments. If this pressure is absent and overlapping loops do not act as shortcuts in the electrical path, the mechanism of sliding contacts and changing path lengths is no longer applicable, and no resistance changes are observed. Considering our interpretation that the sliding of overlapping loops contacts is responsible for obtaining resistance changes, we could interpret the observed knit density effects by realizing that in closer knitted structures the sliding may be partially impaired by adjacent yarns. The larger the NP, the more space for contact point sliding and, consequently, the larger resistance change and gauge factor [25].

The hysteresis values are affected not only by the NP number but also by the position of the conductive yarn. To understand the reasoning behind achieving less hysteresis sensors by positioning conductive yarn inside the structure, we need to understand the loop structure under deformation. Resistance changes due to stretching a knitted structure can in principle be due to both the deformation of the structure and to the stretching of the conductive yarns itself. However, due to the large loops in the structure and the relatively high stiffness of the conductive yarns, the structural deformation will be the dominant part. Only at extremely large deformations (above 70%), the loop lengths are sufficiently straightened up to allow the loading and stretching of the conductive yarns. Note that this type of loading may cause cracks and decrease the adhesion between silver and polyamide in the silver coating, and thus compromises the long-term sensor reliability [26]. The fact that this type of yarn stretching in our 1×1 rib structure only occurs at extremely high deformations is therefore highly beneficial for the sensor reliability.

In Figure 14, we depict how the co-knitting of a conductive yarn on top of a non-conductive one can result in a structure in which the conductive yarns end up on the inside. Note that this type of configuration is typical for the 1×1 rib structure and is not observed for other knitting stitches. When stretched out, the conductive parts of the interlaced loops make contact and start to slide relative to each other which causes the resistance change responsible for the sensor function [27]. In general, when the fabric is stretched, the intra-yarn contact points are pulled apart resulting in increased resistance, whereas the inter-yarn contact points are pulled together leading to reduced resistance.



Figure 14. (a) The illustration of the knitted sample which conductive yarn inserted inside and elastic yarn positioned outside (CI), (b) Representation of the unfolded loops in a course which shows the relative position of the conductive (black line) and elastic (grey line) yarns.

Knitted sensors with a variety of conductive yarns show different sensor performances. Since the elastic and conductive yarn is inserted into the structure together, the yarn thickness can be another parameter that affects the performance. All yarn thicknesses were estimated using an image analysis program and the thickness of the elastic yarn E_1 , as well as the six conductive yarns, are listed in Table 4. From this, we can conclude that the highest

sensitivity values can be achieved when the conductive yarns have comparable thickness compared to the elastic yarn. Note that the difference between the Shieldex yarns and Amann yarns is that Shieldex yarns consist of only silver coated nylon filaments, whereas Amann yarns are hybrid filaments with polyester fibers.

In the results presented until now, the best performing sensor was the one with a gauge factor and hysteresis of 1.19 and 0.03, respectively. Our developed sensor can be compared with the other research in literature as shown in Table 5. In addition, these types of sensors are suitable with high signal integrity required applications such as a respiration sensor or finger monitoring applications [28]. Higher gauge factors were observed for the series, as seen in Figure 6 at around 1.91 and for the series with four courses at around 2.10 (see Figure 11). Such that the NP₁₅ sensor with lower resistance and high elasticity can be used for application in which pauses are needed during the middle of motion monitoring such as dance movements [14].

Table 5. The performance comparison of previous literature studies and this study.

Ref.	Knit Type	Conductive Material	Non-Conductive Material	GF	Hysteresis	WR
Atalay (2013) [10]	Interlock	235 dtex Silver-Nylon	800 dtex elastic yarn	3.75	0.10	10–40%
Atalay (2014) [29]	Interlock	Silver-Nylon	800 dtex elastic yarn	3.44	0.08	>40%
Tognetti (2014) [30]	Intersia	Carbon filled nylon	Lycra	6.7	0.14	>10%
Raji (2018) [15]	1 × 1 Rib	Silver-Nylon	Nylon covered spandex	1.25	-	32.8
Raji (2018) [15]	1 × 2 Rib	Silver-Nylon	Nylon covered spandex	1.50	-	25.3
Raji (2018) [15]	1 × 3 Rib	Silver-Nylon	Nylon covered spandex	1.60	-	31.7
Oks (2014) [31]	Plain	Silver-Nylon	Elastane, Pes, Cotton	10	0.10	5–10%
Chia (2021) [20]	1 × 1 Rib	235 dtex Silver-Nylon	Spandex yarn	1.36	-	20%
Yang (2009) [32]	1 × 1 Rib	Bare SS	-	-1.1	-	50%
Our Study (2022)	1 × 1 Rib	235 dtex Sil-Ny, 600 Ω/m	Nylon- Lycra	1.19	0.03	40%

5. Conclusions

This paper investigates the effect of structure and process parameters on knitted strain sensor performance by conducting a systematical study. Knitted strain sensors have the potential to be used in various applications for body movement monitoring and therefore they should have specific features in terms of sensitivity and stability.

The findings of this study can be summarized in several points:

- The separation of the loops within the knitted structure produced with lower NPs such as 6, 7 and 8 cannot be achieved directly because of the tightness of the samples. At higher NP values of 12 and 15, the sensor starts to respond at higher strain values thanks to an improved elastic response for strains up to 40%.
- A manufacturing technique in which the sensor properties, especially the hysteresis values, can be reduced and controlled in knitted sensors has been reported for the first time. By positioning the conductive yarns inside the 1 × 1 rib structure, a knitted strain sensor with linear performance and a gauge factor of 1.19 and negligible hysteresis of 0.03 was developed.
- The effect of yarn positioning on different types of conductive yarns in terms of hysteresis was also proved. For both S₁ and S₂ yarns, the hysteresis values have decreased for different conductive course numbers. The lowest hysteresis values were achieved for a 2-course sample of S₁ yarn and 3- or 4- course samples of S₂ yarn.
- The performance of sensors made with different conductive yarns was evaluated, and those with lower initial resistance reported higher gauge factors for S-type yarns.
- The highest sensitivity values can be achieved when the conductive yarns have comparable thickness compared to the elastic yarn. Thinner yarns result in poor sensing performance.

Supplementary Materials: The following supporting information can be downloaded at: <https://www.mdpi.com/article/10.3390/s22197688/s1>.

Author Contributions: B.B. conceived the study and carried out the testing; J.J.F.v.D. and L.P. contributed to the sample preparation and technical support; S.G. and K.M.B.J. supervised and reviewed the manuscript. All authors have read and agreed to the published version of the manuscript.

Funding: Beyza Bozali is supported by the Turkish Ministry of National Education for her PhD studies.

Institutional Review Board Statement: Not applicable.

Informed Consent Statement: Not applicable.

Data Availability Statement: The data presented in this study are available on request from the corresponding author. The data are not publicly available due to patent is pending.

Conflicts of Interest: The authors declare no conflict of interest.

References

1. Lee, H.J.; Hwang, S.H.; Yoon, H.N.; Lee, W.K.; Park, K.S. Heart rate variability monitoring during sleep based on capacitively coupled textile electrodes on a bed. *Sensors* **2015**, *15*, 11295–11311. [[CrossRef](#)] [[PubMed](#)]
2. Niu, B.; Hua, T.; Hu, H.; Xu, B.; Tian, X.; Chan, K.; Chen, S. A highly durable textile-based sensor as a human-worn material interface for long-term multiple mechanical deformation sensing. *J. Mater. Chem. C* **2019**, *7*, 14651–14663. [[CrossRef](#)]
3. Maity, S.; Chatterjee, A. Conductive polymer-based electro-conductive textile composites for electromagnetic interference shielding: A review. *J. Ind. Text.* **2018**, *47*, 2228–2252. [[CrossRef](#)]
4. Amjadi, M.; Kyung, K.U.; Park, I.; Sitti, M. Stretchable, skin-mountable, and wearable strain sensors and their potential applications: a review. *Adv. Funct. Mater.* **2016**, *26*, 1678–1698. [[CrossRef](#)]
5. Ma, R.; Lee, J.; Choi, D.; Moon, H.; Baik, S. Knitted fabrics made from highly conductive stretchable fibers. *Nano Lett.* **2014**, *14*, 1944–1951. [[CrossRef](#)]
6. Molinaro, N.; Massaroni, C.; Presti, D.L.; Saccomandi, P.; Di Tomaso, G.; Zollo, L.; Perego, P.; Andreoni, G.; Schena, E. Wearable textile based on silver plated knitted sensor for respiratory rate monitoring. In Proceedings of the 40th Annual International Conference of the IEEE Engineering in Medicine and Biology Society (EMBC), Honolulu, HI, USA, 17–21 July 2018; pp. 2865–2868.
7. Park, S.Y.; Lee, J.H. Machine Embroidered Sensors for Limb Joint Movement-Monitoring Smart Clothing. *Sensors* **2021**, *21*, 949. [[CrossRef](#)]
8. Tangsirinaruenart, O.; Stylios, G. A novel textile stitch-based strain sensor for wearable end users. *Materials* **2019**, *12*, 1469. [[CrossRef](#)]
9. Zhao, K.; Niu, W.; Zhang, S. Highly stretchable, breathable and negative resistance variation textile strain sensor with excellent mechanical stability for wearable electronics. *J. Mater. Sci.* **2020**, *55*, 2439–2453. [[CrossRef](#)]
10. Atalay, O.; Kennon, W.R.; Husain, M.D. Textile-based weft knitted strain sensors: Effect of fabric parameters on sensor properties. *Sensors* **2013**, *13*, 11114–11127. [[CrossRef](#)]
11. Larrabee, W.F., Jr. A finite element model of skin deformation. I. Biomechanics of skin and soft tissue: A review. *Laryngoscope* **1986**, *96*, 399–405.
12. Gibbs, P.T.; Asada, H. Wearable conductive fiber sensors for multi-axis human joint angle measurements. *J. Neuroeng. Rehabil.* **2005**, *2*, 1–18. [[CrossRef](#)] [[PubMed](#)]
13. Atalay, O.; Tuncay, A.; Husain, M.D.; Kennon, W.R. Comparative study of the weft-knitted strain sensors. *J. Ind. Text.* **2017**, *46*, 1212–1240. [[CrossRef](#)]
14. Liang, A.; Stewart, R.; Bryan-Kinns, N. Analysis of sensitivity, linearity, hysteresis, responsiveness, and fatigue of textile knit stretch sensors. *Sensors* **2019**, *19*, 3618. [[CrossRef](#)]
15. Raji, R.K.; Miao, X.; Zhang, S.; Li, Y.; Wan, A. Influence of rib structure and elastic yarn type variations on textile piezoresistive strain sensor characteristics. *Fibres Text. East. Eur.* **2018**, *26*, 24–31. [[CrossRef](#)]
16. Xie, J.; Long, H.; Miao, M. High sensitivity knitted fabric strain sensors. *Smart Mater. Struct.* **2016**, *25*, 105008. [[CrossRef](#)]
17. Raji, R.K.; Miao, X.; Zhang, S.; Li, Y.; Wan, A.; Boakye, A. Knitted piezoresistive strain sensor performance, impact of conductive area and profile design. *J. Ind. Text.* **2020**, *50*, 616–634. [[CrossRef](#)]
18. Jansen, K. Performance evaluation of knitted and stitched textile strain sensors. *Sensors* **2020**, *20*, 7236. [[CrossRef](#)] [[PubMed](#)]
19. Isaia, C.; McMaster, S.; McNally, D. The effect of washing on the electrical performance of knitted textile strain sensors for quantifying joint motion. *J. Ind. Text.* **2022**, *51*, 8528S–8548S [[CrossRef](#)]
20. Chia, P.Z.; Gupta, U.; Tan, Y.Y.; Lau, J.L.; Ahmed, A.; Soh, G.S.; Low, H.Y. Effect of Stitch Pattern on the Electrical Properties of Wale-wise Knitted Strain Sensors and Interconnects. In Proceedings of the IEEE Sensors, Avignon, France, 28–31 March 2021; pp. 1–4.
21. Li, Y.; Miao, X.; Chen, J.Y.; Jiang, G.; Liu, Q. Sensing performance of knitted strain sensor on two-dimensional and three-dimensional surfaces. *Mater. Des.* **2021**, *197*, 109273. [[CrossRef](#)]

22. Dupler, E.; Dunne, L.E. Effects of the textile-sensor interface on stitched strain sensor performance. In Proceedings of the 23rd International Symposium on Wearable Computers, London, UK, 9–12 September 2019; pp. 45–53.
23. Xie, J.; Long, H. Investigation on the relation between structure parameters and sensing properties of knitted strain sensor under strip biaxial elongation. *J. Eng. Fibers Fabr.* **2015**, *10*, 166–178. [[CrossRef](#)]
24. Arbataitis, E.; Mikucioniene, D.; Halavska, L. Flexible Theoretical Calculation of Loop Length and Area Density of Weft-Knitted Structures: Part I. *Materials* **2021**, *14*, 3059. [[CrossRef](#)]
25. Tohidi, S.D.; Zille, A.; Catarino, A.P.; Rocha, A.M. Effects of base fabric parameters on the electro-mechanical behavior of piezoresistive knitted sensors. *IEEE Sensors J.* **2018**, *18*, 4529–4535. [[CrossRef](#)]
26. Ankhili, A.; Zaman, S.U.; Tao, X.; Cochrane, C.; Koncar, V.; Coulon, D. How to connect conductive flexible textile tracks to skin electrocardiography electrodes and protect them against washing. *IEEE Sensors J.* **2019**, *19*, 11995–12002. [[CrossRef](#)]
27. Li, L.; Liu, S.; Ding, F.; Hua, T.; Au, W.M.; Wong, K.S. Electromechanical analysis of length-related resistance and contact resistance of conductive knitted fabrics. *Text. Res. J.* **2012**, *82*, 2062–2070. [[CrossRef](#)]
28. Ryu, H.; Park, S.; Park, J.J.; Bae, J. A knitted glove sensing system with compression strain for finger movements. *Smart Mater. Struct.* **2018**, *27*, 055016. [[CrossRef](#)]
29. Atalay, O.; Kennon, W.R.; Demirok, E. Weft-knitted strain sensor for monitoring respiratory rate and its electro-mechanical modeling. *IEEE Sensors J.* **2014**, *15*, 110–122. [[CrossRef](#)]
30. Tognetti, A.; Lorussi, F.; Mura, G.D.; Carbonaro, N.; Pacelli, M.; Paradiso, R.; Rossi, D.D. New generation of wearable goniometers for motion capture systems. *J. Neuroeng. Rehabil.* **2014**, *11*, 1–17. [[CrossRef](#)]
31. Oks, A.; Katashev, A.; Litvak, J. Knitted resistive fabric: properties and applications. *Mater. Sci. Text. Cloth. Technol.* **2014**, *9*, 28–33. [[CrossRef](#)]
32. Yang, K.; Song, G.I.; Zhang, L.; Li, L.W. Modelling the electrical property of 1×1 rib knitted fabrics made from conductive yarns. In Proceedings of the Second International Conference on Information and Computing Science, Manchester, UK, 21–22 May 2009; Volume 4, pp. 382–385.